THE JOURNAL OF BIOLOGICAL CHEMISTRY VOL. 283, NO. 22, pp. 15451–15459, May 30, 2008

Metabolism of the Folate Precursor *p*-Aminobenzoate in Plants

*GLUCOSE ESTER FORMATION AND VACUOLAR STORAGE**

Received for publication, November 26, 2007, and in revised form, March 7, 2008 Published, JBC Papers in Press, April 2, 2008, DOI 10.1074/jbc.M709591200

Aymerick Eudes[‡1], Gale G. Bozzo[‡1], Jeffrey C. Waller[‡], Valeria Naponelli[§], Eng-Kiat Lim[¶], Dianna J. Bowles[¶], Jesse F. Gregory III[§], and Andrew D. Hanson[‡2]

From the Departments of [‡]Horticultural Sciences and [§]Food Science and Human Nutrition, University of Florida, Gainesville, Florida 32611 and the [¶]Centre for Novel Agricultural Products, Department of Biology, University of York, York YO10 5DD, United Kingdom

Plants produce *p*-aminobenzoate (*p*ABA) in chloroplasts and use it for folate synthesis in mitochondria. In plant tissues, however, *p*ABA is known to occur predominantly as its glucose ester (*p*ABA-Glc), and the role of this metabolite in folate synthesis has not been defined. In this study, the UDP-glucose:*p*ABA acyl-glucosyltransferase (*p*AGT) activity in *Arabidopsis* extracts was found to reside principally (95%) in one isoform with an apparent K_m for *p*ABA of 0.12 mM. Screening of recombinant *Arabidopsis* UDP-glycosyltransferases identified only three that recognized *p*ABA. One of these (UGT75B1) exhibited a far higher k_{cat}/K_m value than the others and a far lower apparent K_m for *p*ABA (0.12 mM), suggesting its identity with the principal enzyme *in vivo*. Supporting this possibility, ablation of UGT75B1 reduced extractable *p*AGT activity by 95%, *in vivo* [^{14}C]*p*ABA glucosylation by 77%, and the endogenous *p*ABA-Glc/*p*ABA ratio by 9-fold. The K_{eq} for the *p*ABA esterification reaction was found to be 3×10^{-3}. Taken with literature data on the cytosolic location of *p*AGT activity and on cytosolic UDP-glucose/UDP ratios, this K_{eq} value allowed estimation that only 4% of cytosolic *p*ABA is esterified. That *p*ABA-Glc predominates *in planta* therefore implies that it is sequestered away from the cytosol and, consistent with this possibility, vacuoles isolated from [^{14}C]*p*ABA-fed pea leaves were estimated to contain ≥88% of the [^{14}C]*p*ABA-Glc formed. In total, these data and the fact that isolated mitochondria did not take up [^{3}H]*p*ABA-Glc, suggest that the glucose ester represents a storage form of *p*ABA that does not contribute directly to folate synthesis.

Tetrahydrofolate and its derivatives (folates) are essential cofactors for one-carbon reactions in almost all organisms, but are made only by plants and microbes (1, 2). Folates are tripartite molecules comprising pterin, *p*-aminobenzoate (*p*ABA),[3] and glutamate moieties (Fig. 1*A*), and folate synthesis in plants involves three subcellular compartments (Fig. 1*B*). The pterin moiety is synthesized in the cytosol, *p*ABA is synthesized in chloroplasts, and the two are coupled together, reduced, and glutamylated in mitochondria (3). Although folate synthesis itself is fairly well understood, the metabolism and transport of the pathway intermediates, *p*ABA and pterins, are not. Such ignorance impedes rational engineering to enhance folate levels in food crops for improved human health (4).

After its formation in chloroplasts, *p*ABA must transit the cytosol before entering mitochondria for folate synthesis (Fig. 1*B*). As a hydrophobic weak acid, *p*ABA can cross membranes by simple diffusion according to pH and concentration gradients (5). However, *p*ABA has been shown to occur in plants mainly as its glucose ester (*p*ABA-Glc), which is hydrophilic and almost certainly cannot readily diffuse across membranes (6). Because free *p*ABA is present only at low concentrations it is entirely conceivable that mitochondria import *p*ABA-Glc and then hydrolyze it to *p*ABA for folate synthesis (Fig. 1*B*). Nothing is known about this issue or, more generally, about transport of aromatic conjugates by plant mitochondria (7).

Nor is it clear whether *p*ABA-Glc is restricted to the cytosol. Vacuoles are well known to import glucose conjugates of aromatic compounds (8), and experiments with tissue cultures given megadoses of *p*ABA suggest that some of the *p*ABA-Glc formed is probably in vacuoles. Specifically, cell suspension cultures of *Solanum laciniatum* supplied with 2.5 mM *p*ABA accumulate levels of *p*ABA-Glc that, from osmotic considerations, appear too high to be confined to the cytosol (6, 9). These data invite the questions of whether *p*ABA-Glc import into vacuoles indeed occurs (Fig. 1*B*), and, if so, whether it is a normal process or a pharmacological aberration.

*p*ABA-Glc formation is known to be a reversible reaction mediated by cytosolic UDP-glucose: *p*ABA acyl-glucosyltransferase (*p*AGT) activity (6) but no protein with this activity has yet been identified. However, a prediction about *p*AGT can be made from bioinformatics. The *Arabidopsis thaliana* (hereafter, *Arabidopsis*) genome encodes >100 UDP-glucosyltransferases (UGTs) that fall into 14 phylogenetically distinct groups (A to N) (10). Prior work on recombinant UGTs has shown that

* This work was supported, in whole or in part, by National Institutes of Health Grant R01 GM071382. This work was also supported by an endowment from the C. V. Griffin, Sr. Foundation. The costs of publication of this article were defrayed in part by the payment of page charges. This article must therefore be hereby marked "*advertisement*" in accordance with 18 U.S.C. Section 1734 solely to indicate this fact.

[1] These authors contributed equally to this work.

[2] To whom correspondence should be addressed: University of Florida, Horticultural Sciences Dept., P.O. Box 110690, Gainesville, FL 32611-0690. Fax: 352-392-5653; E-mail: adha@ufl.edu.

[3] The abbreviations used are: *p*ABA, *p*-aminobenzoic acid; *p*ABA-Glc, *p*-aminobenzoate β-D-glucose ester; *p*AGT, UDP-glucose:*p*ABA acyl-glucosyltransferase; HPLC, high performance liquid chromatography; UGT, UDP-glucosyltransferase; MOPS, 4-morpholinepropanesulfonic acid; MES, 4-morpholineethanesulfonic acid.

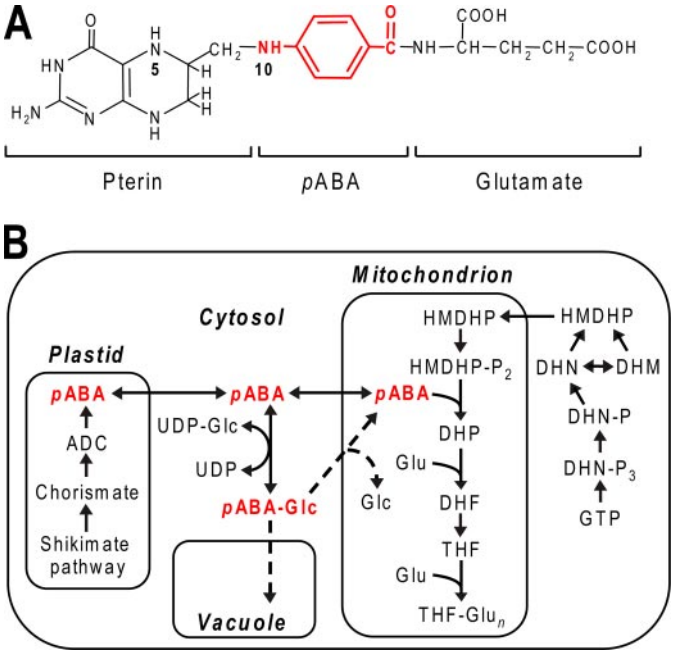

FIGURE 1. **Folate structure and compartmentation of the plant folate synthesis pathway.** *A*, tetrahydrofolate, with the *p*ABA moiety colored *red*. Other natural folates have one-carbon units attached to the N5 and/or N10 positions. A γ-linked polyglutamyl tail of up to about six residues is usually attached to the first glutamate. *B*, the currently accepted scheme of folate biosynthesis in plants, showing subcellular locations of biosynthetic steps and of *p*ABA esterification (highlighted in *rose*) and hypothetical transport steps for *p*ABA-Glc into the mitochondrion and vacuole tested in this study (*dashed arrows*). Note that polyglutamylation of folates also occurs in the cytosol and plastids. *ADC*, aminodeoxychorismate; *DHF*, dihydrofolate; *DHM*, dihydromonapterin; *DHN*, dihydroneopterin; *DHP*, dihydropteroate; *HMDHP*, hydroxymethyldihydropterin; *-P*, phosphate; *-P_2*, pyrophosphate, *-P_3*, triphosphate; *THF*, tetrahydrofolate; *UDP-Glc*, UDP-glucose.

enzymes that form glucose esters with various benzoates belong to group L (11), making it likely that enzymes with *p*AGT activity are in this group.

In this study, we partially characterized *p*AGT activity extracted from *Arabidopsis*, screened *Arabidopsis* group L UGTs for *p*AGT activity, and biochemically characterized the three most active enzymes. This work implicated UGT75B1 as the main source of *p*AGT activity *in planta*, for which supporting evidence came from reverse-genetics. Radiolabeling approaches were used to investigate vacuolar and mitochondrial uptake of *p*ABA-Glc, and to estimate K_{eq} for the esterification reaction. The data strongly suggest that *p*ABA-Glc is not taken up by mitochondria but rather represents a vacuolar storage form of *p*ABA that does not contribute directly to folate synthesis.

EXPERIMENTAL PROCEDURES

Chemicals and Reagents—[*Ring*-^{14}C]*p*ABA (55 mCi mmol^{-1}), [3,5-^{3}H]*p*ABA (26.2 Ci mmol^{-1}), [3′,5′,7,9-^{3}H]folic acid diammonium salt (43.2 Ci mmol^{-1}), and [2,3,4,5-^{3}H]proline (72.5 Ci mmol^{-1}) were from Moravek Biochemicals (Brea, CA). [^{3}H]Proline and [^{14}C]*p*ABA (when used for K_{eq} estimation) were purified as follows. [^{3}H]Proline (108 μCi) was dried *in vacuo*, redissolved in 5 μl of water and applied to a 1-cm origin on a 10-cm cellulose TLC plate, which was developed in butanol/acetic acid/water (60:15:25, v/v/v). The proline zone (R_f = 0.3) was scraped from the plate and eluted with 3 × 200 μl H_2O. [^{14}C]*p*ABA (2.2 μCi) was dried *in vacuo*, redissolved in 50 μl of water, and separated by HPLC using a Discovery 5-μm C18 (250 × 4.6 mm, Supelco) column; detection was by fluorescence (270 nm excitation, 350 nm emission). The column was eluted (1 ml min^{-1}) with 0.5% acetic acid/methanol (80:20, v/v). Unlabeled *p*ABA-Glc was prepared as described (6). [^{3}H]*p*ABA-Glc was synthesized enzymatically from [^{3}H]*p*ABA (10 μCi, 0.38 nmol), which was dried *in vacuo* and redissolved in 8 μl of 25 mM Tris-HCl, pH 7.5. The reaction (10-μl final volume) contained [^{3}H]*p*ABA, 0.4 μg of UGT75B1, 4 mM UDP-glucose, and 14 mM 2-mercaptoethanol, and was incubated at 30 °C for 90 min. The reaction was stopped by freezing in liquid N_2. Upon thawing, the [^{3}H]*p*ABA-Glc product was isolated by HPLC as described below. The radiochemical yield was 18%, and radiochemical purity was >99%. UDP-glucose was purchased from Sigma and checked for purity by HPLC (12); purity was determined to be >99%. Dowex (AG) resins were from Bio-Rad. TLC plates were from Merck (Darmstadt, Germany). Protein chromatography columns were from GE Healthcare (Piscataway, NJ).

Plant Materials—Arabidopsis (ecotypes Columbia-0 and Landsberg *erecta*) plants were grown at 23–28 °C in 12-h days (80 μmol m^{-2} s^{-1}) in potting soil irrigated with water. For root production, plants were grown hydroponically (13). Pea (*Pisum sativum* cv. Laxton's Improved Progress 9) plants were grown as described (14). Cauliflower was obtained from a local market. The UGT75B1 mutant (line MGT.6017) was identified in the *Arabidopsis* (ecotype Landsberg *erecta*) Cold Spring Harbor Genetrap transposon insertion collection. Wild type or homozygous mutant segregants were identified by PCR using gene-specific primers located 5′ or 3′ of the *Ds* insertion (5′-GGCTAGACTCGAAAACAGAGT-3′ and 5′-CCTCCTCT-GCTTCACACAAG-3′, respectively) and a *Ds*-specific primer (5′-CGCTGGCCTGCCCAACC-3′). Genomic DNA was extracted as described (15). The insertion site was confirmed by sequencing the amplicon from mutant homozygotes. Homozygous mutant and wild-type segregants were selfed, and their progeny were used for experiments.

Production and Purification of Recombinant UGTs—Procedures for *Escherichia coli* expression and protein isolation used to screen glutathione *S*-transferase-UGT fusions for *p*AGT activity were as described (16). For further analysis of UGT75B1, UGT74F1, and UGT74F2, fusion constructs were introduced into *E. coli* BL21-CodonPlus (DE3)-RIPL cells (Stratagene), which were grown at 37 °C in LB medium until the A_{600} reached 0.6. The temperature was then lowered to 25 °C, and isopropyl-D-thiogalactopyranoside was added (final concentration, 0.5 mM). Incubation was continued for 4 h at 25 °C. Subsequent procedures were at 0–4 °C. Cells from 100-ml cultures were pelleted, resuspended in 1 ml of phosphate-buffered saline, and broken in a Mini-Bead Beater (Biospec, Bartlesville, OK). Lysates were cleared by centrifugation (10,000 × *g*, 10 min). To remove co-purifying contaminant proteins, lysates were incubated with 8 M urea-denatured *E. coli* proteins (17). The mixture was centrifuged at 1,500 × *g* for 10 min, and the supernatant was mixed with glutathione-Sepharose resin and purified recombinant UGT recovered as described (16). The

purified UGTs were desalted (100 mM Tris-HCl, pH 8.0) on Sephadex G-25 mini-spin columns, flash-frozen, and stored at −80 °C. Protein was estimated by the Bradford method (18) using bovine serum albumin as the standard. Recombinant proteins were analyzed by SDS-PAGE (19).

Extraction and Separation of Arabidopsis pAGT Activity—Tissues were pulverized in liquid N_2. Protein extraction and purification steps were at 0–4 °C. For tests of *p*AGT activity in various tissues, protein was extracted in 50 mM Tris-HCl, pH 8.0, containing 10 mM 2-mercaptoethanol and 30 mg/ml polyvinylpolypyrrolidone (2 ml/g fresh weight). The extract was centrifuged (10,000 × *g*, 20 min), and the supernatant was filtered through a layer of Miracloth, then desalted on a PD-10 column equilibrated in 50 mM Tris-HCl, pH 7.5, containing 10% (v/v) glycerol, and 10 mM 2-mercaptoethanol. For partial purification of *p*AGT activity, the clarified extract from leaves (13 g) of 5-week-old Columbia-0 plants was brought to 80% saturation with $(NH_4)_2SO_4$. After stirring for 30 min and centrifuging (13,000 × *g*, 20 min), the pellet was redissolved in 4.8 ml of 25 mM Tris-HCl, pH 7.5, containing 5 mM 2-mercaptoethanol (Buffer A) and desalted on PD-10 columns equilibrated with Buffer A. The solution was applied (1 ml min^{-1}) to a Mono Q HR 5/5 column equilibrated with Buffer A, and the column was washed with this buffer until the A_{280} of the effluent fell to zero. *p*AGT activity was eluted (1 ml min^{-1}) with a 15-ml gradient of 0–500 mM KCl in Buffer A, collecting 0.3-ml fractions. Active fractions were pooled, brought to 10% (v/v) glycerol, frozen in liquid N_2, and stored at −80 °C until use.

pAGT Assays—Activities were measured at 30 °C; product formation was linear with time and amount of protein. Initial screening of recombinant UGTs for *p*AGT activity was in assay mixtures (200 μl) containing 1 μg of protein (not previously frozen and thawed), 50 mM Tris-HCl, pH 7.0, 14 mM 2-mercaptoethanol, 2.5 mM UDP-glucose, and 1 mM *p*ABA. Reactions were incubated for 30 min, stopped by adding 20 μl of trichloroacetic acid (240 mg ml^{-1}), flash-frozen, and stored at −20 °C before reverse-phase HPLC analysis as described (11). Kinetic constants of UGT75B1, UGT74F1, and UGT74F2 were measured on purified proteins that had been frozen once, using assay mixtures (20 μl) containing 25 mM Tris-HCl, pH 7.5, 100 ng of protein, 4 mM UDP-glucose, and the indicated amounts of [^{14}C]*p*ABA and glycerol. Assays were stopped in liquid N_2, then applied to AG 4-X4 (OH^-) columns to quantify [^{14}C]*p*ABA-Glc formation as described (6). A freeze-thaw cycle reduced *p*AGT specific activities by up to 10-fold, but use of frozen enzymes was deemed acceptable as it allowed analysis of all three UGTs at once. For *Arabidopsis p*AGT activity, standard reaction mixtures (final volume 20 μl) contained 25 mM Tris-HCl, 4–18 μg of protein, 45 μM [^{14}C]*p*ABA, and 4 mM UDP-Glc; [^{14}C]*p*ABA-Glc formation was measured as above. For fractions from Mono Q chromatography, assay mixtures were applied to 1-ml columns of AG 4-X4 ($C_2H_5COO^-$), from which [^{14}C]*p*ABA-Glc was eluted with 20 ml of water and counted.

Estimation of K_{eq}—The K_{eq} for the *p*ABA esterification reaction was estimated by measuring [^{14}C]*p*ABA-Glc formation. Assay mixtures (20 μl final volume) contained 1.5 μg of purified glutathione *S*-transferase-fused UGT75B1, 10 nmol of UDP-glucose, 9.25 nmol of unlabeled *p*ABA, and 41.3 nCi (0.75 nmol) of purified [^{14}C]*p*ABA in 50 mM MOPS-NaOH, pH 7.5, or 50 mM Tris-HCl, pH 7.5. Reactions were incubated at 30 °C for various times, after which the [^{14}C]*p*ABA-Glc product was quantified by TLC as described (6).

[^{14}C]pABA Metabolism in Arabidopsis in Vivo—The surface of the midrib was shaved from the abaxial surface of *Arabidopsis* leaves. A 3-μl droplet containing 68 nCi (1.23 nmol) of [^{14}C]*p*ABA and 939 nmol of unlabeled *p*ABA dissolved in water was applied to the cut surface of each leaf. Leaves were incubated in Petri dishes for 3 h at 24 °C in the light (150 μmol m^{-2} s^{-1}) and then shaken (100 rpm) for 15 min in 5 ml of 0.1 mM *p*ABA to remove non-absorbed label. Tissues were extracted by grinding in 2 ml of semifrozen methanol. Aliquots (120 μl) of the methanol extract were separated by TLC as described (6); radioactive zones were detected by autoradiography and scraped from the plate for scintillation counting.

Determination of Free and Total pABA—Arabidopsis wild-type and UGT75B1 mutant leaf tissue samples (0.4 g fresh weight) were extracted and analyzed by HPLC for free and total *p*ABA as described (6). Esterified *p*ABA was calculated as (total *p*ABA − free *p*ABA). Data were corrected for recovery using free *p*ABA spikes.

Pea Leaf Vacuole Experiments—The surface of the midrib was shaved from the abaxial surface of pea leaflets (1 g, 20–22 leaflets). A solution of [^{14}C]*p*ABA (0.30–0.33 μCi, 5.4–6.0 nmol) dissolved in 3 μl of water was applied to the cut surfaces. Leaflets were incubated in Petri dishes for 3 h at 24 °C in light (150 μmol m^{-2} s^{-1}). After the incubation, protoplasts were prepared from the [^{14}C]*p*ABA-fed leaflets together with unlabeled pea leaflets (24 g) following a 5-h digestion as described (20) except that the centrifugation step used to harvest protoplasts included a cushion of 50% (v/v) Percoll in 10 mM MES-NaOH, pH 7.0, 0.5 M sorbitol, 5 mM $CaCl_2$, 0.5 mg/ml polyvinylpyrrolidone-40. The protoplast layers were adjusted to 13% Percoll in the same buffer and purified on a three-step sucrose-sorbitol gradient as described (21). Vacuoles were prepared from lysed protoplasts (20) after adding to the lysate unlabeled folic acid to a final concentration of 50 μM and 2–25 μCi (0.05–0.58 nmol) of [^{3}H]folic acid. Marker enzymes were extracted and assayed as described (20). Vacuolar yield was quantified by counting protoplast and vacuole preparations using a hemocytometer, and by measuring α-mannosidase activity (22). The purity of the vacuole fraction was attested by the absence of chlorophyll and by the very low recovery (<0.5%) of mitochondrial (fumarase) and stromal (NADP-linked glyceraldehyde-3-phosphate dehydrogenase) marker enzyme activities (23). The ^{3}H and ^{14}C contents of protoplast lysate and vacuole fractions were determined by scintillation counting. Before HPLC analysis of the vacuolar ^{14}C label, ultrafiltration using a Centricon-10 (Millipore, Billerica, MA) was used to remove Ficoll. The ultrafiltrate was concentrated 2-fold *in vacuo* before HPLC analysis. HPLC separation was carried out on a Discovery 5-μm C_{18} (250 × 4.6 mm, Supelco); detection was by absorbance at 295 nm or fluorescence (270 nm excitation, 350 nm emission). The column was eluted (1 ml min^{-1}) with 10% acetonitrile/0.1% trifluoroacetic acid in water; fractions (0.33 ml) were collected, and the radioactivity counted.

Mitochondrial [^{3}H]pABA-Glc Transport Tests—Mitochondria were isolated from 500 g of cauliflower florets and purified by Percoll density gradient centrifugation (24). The purified mitochondria were resuspended in transport buffer (25 mM MOPS, pH 7.4, 0.33 M sucrose, 1 mM EDTA, and 1 mM dithiothreitol). Mitochondrial extracts were obtained by freezing in liquid N_2 and thawing at 30 °C (5 cycles), followed by centrifugation at 16,000 × *g* for 10 min at 4 °C. As a quality control, fumarase was assayed in the freshly prepared extract (20); typical activities were 5 μmol min^{-1} mg^{-1} protein. [^{3}H]pABA-Glc transport assays (final volume 500 μl) contained 92 nCi (3.5 pmol) of [^{3}H]*p*ABA-Glc and 1 mM NADH in transport buffer (25). Assays were started by adding mitochondria (330 μg protein) and incubated at 30 °C with magnetic stirring. At intervals, 75-μl aliquots were withdrawn, and mitochondria were harvested on a Whatman cellulose nitrate membrane filter (0.45 μM) using a vacuum filtration device. Filters were washed twice with 2 ml of ice-cold transport buffer, added to 3 ml of Beckman Ready Gel scintillation fluid (Beckman Coulter, Fullerton, CA), equilibrated, and counted. [^{3}H]Proline uptake was measured by the same method using 254 nCi (3.5 pmol) of [^{3}H]proline.

Estimation of Endogenous pABA Production Rate in Arabidopsis—The endogenous *p*ABA production rate in *Arabidopsis* leaves (~2.5 pmol mg^{-1} protein h^{-1}) was estimated from published folate and total *p*ABA contents (6, 14) by assuming a growth rate of 10% per day (26) and a protein content of 10 mg g^{-1} fresh weight.

RESULTS

Organ Distribution and Isoform Complexity of pAGT Activity in Arabidopsis—Because *p*AGT activity has not been studied *ex vivo* in *Arabidopsis*, we first assayed *p*AGT activities in extracts from various organs of ecotype Columbia-0 to determine where *p*AGT is most strongly expressed (Fig. 2*A*). A relatively low *p*ABA concentration (45 μM) was used to mimic the cytosolic free *p*ABA concentration, which can be estimated as ≤45 μM from published data on plant *p*ABA contents (6) and cytosol volume (27). *p*AGT activity was highest in leaves, flowers, and siliques, and was equally high in ecotype Landsberg *erecta* leaves, which were analyzed for comparison (Fig. 2*A*). To investigate *p*AGT isoforms, Columbia leaf activity was fractionated by anion exchange chromatography (Fig. 2*B*). A single major peak of activity eluted at ~220 mM NaCl, and a minor peak (representing ≤5% of the total activity) eluted at ~320 mM. The *p*AGT activity in leaves thus comes mainly from one isoform. Triplicate determinations of the K_m for *p*ABA of the major peak activity gave a value of 0.12 ± 0.02 mM (mean ± S.E.).

Identification and Characterization of Recombinant UGTs with pAGT Activity—Sequences from Group L of the *Arabidopsis* UGT family were expressed as glutathione *S*-transferase fusion proteins in *E. coli*, affinity-purified, and screened for *p*AGT activity by an HPLC assay (11). UGT75B1 had high activity, and UGT74F1 and UGT74F2 had moderate activity; the others had lower activity or none (Fig. 3*A*). The three enzymes with the most activity were kinetically characterized using a sensitive radioassay; the protein preparations used were near homogeneous (Fig. 3*B*). UGT75B1 was the most active enzyme in terms of its k_{cat}/K_m value and had by far the lowest apparent

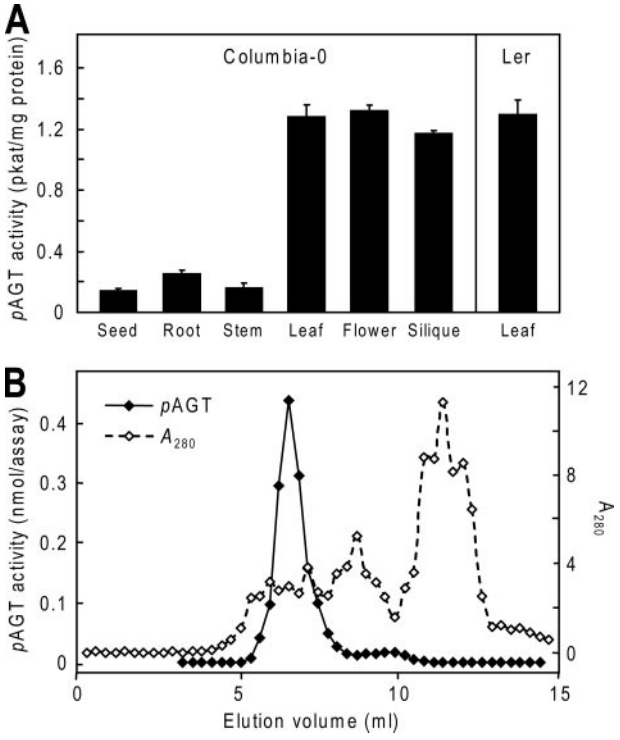

FIGURE 2. ***p*AGT activity in *Arabidopsis*.** *A*, *p*AGT activities in extracts of organs of ecotype Columbia-0. The activity in leaves of Landsberg *erecta* (*Ler*) is shown for comparison. Enzyme assays contained 45 μM *p*ABA and 4 mM UDP-glucose. Values for leaves, flowers, roots, and seeds are means and S.E. for two to four replicates from two or three independent extracts; stem and silique values are for single extracts. *B*, anion exchange chromatography of Columbia-0 leaf proteins, showing one major peak of *p*AGT activity. Ammonium sulfate-precipitated proteins (42 mg) were applied to a 1-ml Mono Q column and eluted with a 0–0.5 M NaCl gradient. Enzyme assays (20 μl final volume) contained 40 μM [^{14}C]*p*ABA (0.8 nmol) and 4 mM UDP-glucose, and were run for 30 min. Enzyme activity is in nmol of *p*ABA-Glc formed per assay.

K_m (Table 1). Significantly, the K_m value of recombinant UGT75B1 was identical (0.12 mM) to that found for the enzyme extracted from *Arabidopsis*. These results strongly imply that UGT75B1 is the major contributor to *p*AGT activity *in planta*.

Insertional Inactivation of UGT75B1—To corroborate the involvement of UGT75B1 in *p*ABA glucosylation *in planta*, the consequence of knocking out expression of the gene was investigated. A *Ds* mutant of the *UGT75B1* gene (*At1g05560*), which is intronless, was identified in the Cold Spring Harbor Genetrap collection, in the Landsberg *erecta* background. The *Ds* insertion is at nucleotide 1238, corresponding to amino acid 412 of the 469-residue protein (Fig. 4*A*). Plants homozygous for this insertion were identified by PCR screening (Fig. 4*B*), and PCR tests of wild-type segregants from the same population confirmed that other *Ds* elements were absent (data not shown). RT-PCR analysis of mutant homozygotes detected a UGT75B1 message with an in-frame stop codon 21 nucleotides after the *Ds* junction. The putative translation product is most unlikely *a priori* to have UGT activity because the missing C-terminal region contains two conserved α-helical domains that subtend the UDP-glucose binding site (28, 29). The *Ds* mutation did not visibly affect germination, growth, or development.

Total *p*AGT activity was assayed in leaf, flower, and silique extracts from mutant plants and wild-type segregants using 45 μM *p*ABA as above (Fig. 4*C*). Extracts from mutant plants dis-

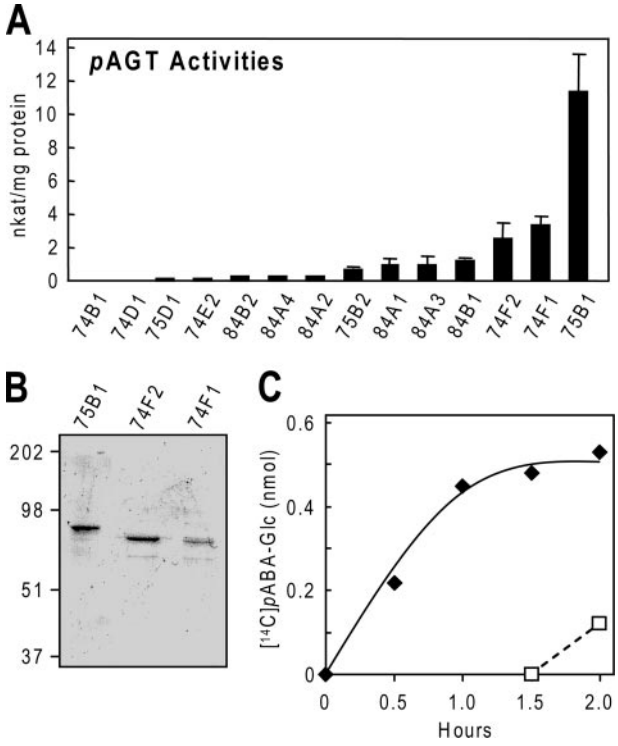

FIGURE 3. **Characterization of *Arabidopsis* group L UGTs and of the esterification reaction.** *A*, *p*AGT activities of 16 members of group L measured using 1 mM *p*ABA and 2.5 mM UDP-glucose. Data are means of three replicates and S.E. For UGT75B1, the activity with UDP-galactose or UDP-glucuronate as sugar donor was found to be negligible (<1% of that with UDP-glucose). *B*, SDS-PAGE analysis of affinity-purified preparations of the three UGTs with the highest *p*AGT activities. Tracks contained 1 μg (UGT75B1, UGT74F2) or 0.5 μg (UGT74F1) of protein. The gel was stained with Coomassie Blue. Running positions of molecular mass markers (kDa) are indicated on the *left*. *C*, progress curve of [^{14}C]*p*ABA-Glc formation in a reaction mixture containing 1.5 μg of purified UGT75B1, 10 nmol of UDP-glucose, 9.25 nmol of unlabeled *p*ABA, and 41.3 nCi (0.75 nmol) of [^{14}C]*p*ABA (*solid symbols* and *line*), in 50 mM MOPS-NaOH, pH 7.5. A second reaction mixture without radiolabel was incubated in parallel with the first for 1.5 h, at which point 41.3 nCi of [^{14}C]*p*ABA was added (*open symbols* and *dotted line*). The formation of [^{14}C]*p*ABA-Glc in this reaction shows that UGT75B1 remained enzymatically active throughout the experiment.

TABLE 1

Kinetic characteristics of *Arabidopsis* UGTs with *p*AGT activity

Enzyme activities were measured radiometrically at pH 7.5 using affinity-purified glutathione *S*-transferase fusion proteins. K_m and k_{cat} values are the means of three replicates ± S.E.

Protein	K_m	k_{cat}	k_{cat}/K_m
	mM	s^{-1}	$mM^{-1}\,s^{-1}$
UGT75B1	0.12 ± 0.01	13.8 ± 0.6	115
UGT74F2	0.92 ± 0.14	8.8 ± 1.1	9.6
UGT74F1	0.85 ± 0.12	10.5 ± 0.2	12.4

played on average a 95% reduction in activity. This strongly indicates that UGT75B1 is the main *p*AGT isoform in all three organs. These results were extended by comparing the capacity of mutant and wild-type leaves to convert [^{14}C]*p*ABA to [^{14}C]*p*ABA-Glc *in vivo*, using a [^{14}C]*p*ABA dose (~20 μmol/g fresh weight) sufficient to ensure that it would not all be esterified during the experiment (6). TLC analysis of labeled metabolites showed that [^{14}C]*p*ABA-Glc formation was drastically (77%) reduced in the mutant (Fig. 4*D*). Consistent with their lower *p*AGT activity, mutant leaves showed significantly ($p < 0.05$) decreased endogenous *p*ABA-Glc levels and increased

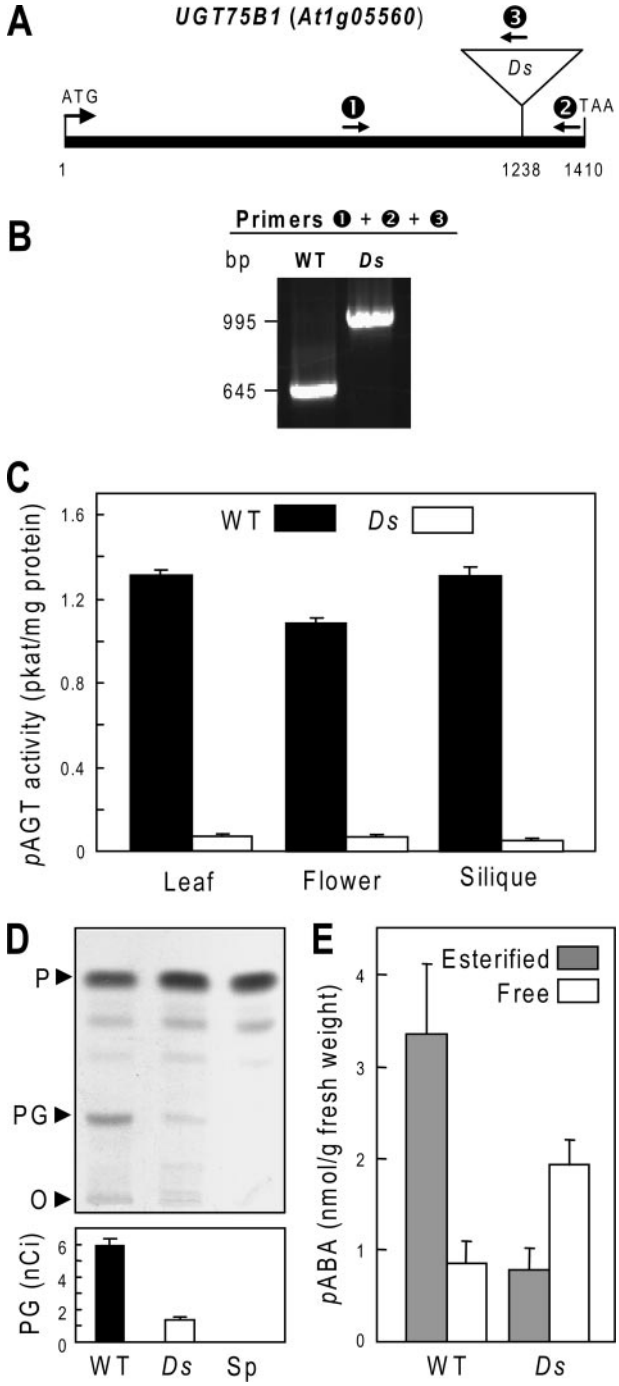

FIGURE 4. **Insertional inactivation of the *UGT75B1* gene (*At1g05560*) in the Landsberg *erecta* background.** *A*, the *UGT75B1* gene (which is intronless), showing the position of the *Ds* insert and of the three PCR primers (*1*, *2*, *3*) used for analysis of genomic DNA. Primer abbreviations: *1*, *UGT75B1*-specific forward primer; *2*, *UGT75B1*-specific reverse primer; *3*, *Ds*-specific reverse primer. *B*, gel separation of PCR products amplified from genomic DNA of homozygous wild type and mutant plants using a mixture of primers *1*, *2*, and *3*. *C*, *p*AGT activities in extracts of leaves, flowers, and siliques of wild type and mutant plants. Values are means and S.E. for two replicates from two independent extracts. *D*, autoradiograph of a TLC separation of extracts of wild type (*WT*) and mutant (*Ds*) leaves (0.14 g) supplied with 52 nCi (2.82 μmol) of [^{14}C]*p*ABA for 3 h. The origin (*O*) and running positions of *p*ABA (*P*) and *p*ABA-Glc (*PG*) standards are indicated. A control sample of unlabeled leaves (*Sp*) spiked with [^{14}C]*p*ABA just before extraction is included. *Bars* below the autoradiograph show the amounts of [^{14}C]*p*ABA-Glc present in the samples; these values are means of four replicates and S.E. *E*, estimation of free and esterified *p*ABA in wild type and mutant leaves. Values are means and S.E. for three samples. The free *p*ABA data are not corrected for the contribution of ester hydrolysis during sample processing.

endogenous free *p*ABA levels, so that the *p*ABA-Glc/*p*ABA ratio fell to 0.4 compared with 3.5 in the wild type (Fig. 4*E*). The total (esterified plus free) endogenous *p*ABA levels did not differ significantly between mutant and wild type.

Measurement of K_{eq} for the Esterification Reaction—The K_{eq} for *p*ABA esterification was estimated by following [^{14}C]*p*ABA-Glc formation in a reaction mixture containing purified recombinant UGT75B1, 10 nmol of unlabeled UDP-glucose, and 10 nmol of *p*ABA containing a tracer amount of ^{14}C (Fig. 3*C*). The reaction appeared to have reached equilibrium at 1.5 h, by which time [^{14}C]*p*ABA-Glc formation had plateaued. To verify that this plateau was not due to enzyme inactivation, a parallel reaction was run with unlabeled substrates, and tracer [^{14}C]*p*ABA was added at 1.5 h. The subsequent formation of [^{14}C]*p*ABA-Glc (Fig. 3*C*, *dotted line*) showed that UGT75B1 remained active throughout the experiment. The quantity of [^{14}C]*p*ABA-Glc present at equilibrium (0.5 nmol) corresponds to a K_{eq} value of 3×10^{-3}. Three similar experiments confirmed this value and showed that the nature of the buffer used (Tris-HCl *versus* MOPS-NaOH) had little if any effect (not shown).

Evidence for Vacuolar Storage of pABA-Glc—To determine whether *p*ABA-Glc enters vacuoles, we used an *in vivo* dual labeling approach based on the ability of leaves to rapidly convert tracer amounts of [^{14}C]*p*ABA to *p*ABA-Glc (6). A small sample of pea leaflets was supplied with a tracer dose of [^{14}C]*p*ABA for 3 h, then mixed with unlabeled leaves and used to prepare mesophyll protoplasts. Vacuoles were then isolated from the protoplasts. Just after protoplasts were lysed to release vacuoles, low specific activity [^{3}H]folic acid was added to the lysate as a marker for contamination of vacuoles by extravacuolar solutes. (The low specific activity of the [^{3}H]folic acid ensured that, if any vacuolar uptake occurred, its ^{3}H content would be negligible. Moreover, tests with vacuolar vesicles showed no detectable [^{3}H]folic acid uptake (not shown).) The ^{14}C and ^{3}H contents of the isolated vacuoles were measured and compared with those of the protoplast lysate, and with the yield of vacuoles assessed by counting and by recovery of the vacuole marker α-mannosidase (30).

In three separate experiments, an average of 8.4% of the ^{14}C present in the protoplast lysate was recovered in purified vacuoles *versus* 0.4% of the ^{3}H (Fig. 5*A*), indicating that 8.0% of the ^{14}C was intravacuolar. Because the mean yield of vacuoles was 10.1% as judged from vacuole numbers and α-mannosidase recovery (Fig. 5*A*), we can calculate that, on average, 79% (range 60–90%) of the ^{14}C was located in vacuoles *in vivo* (Fig. 5*B*), this being a minimum estimate because ^{14}C may have leaked out during isolation. Of the ^{14}C label recovered from vacuoles, HPLC analysis demonstrated that essentially none was in the form of free *p*ABA and that 80% was in the form of *p*ABA-Glc (Fig. 5*C*) so that the [^{14}C]*p*ABA-Glc present in vacuoles was $(0.79 \times 0.8 \times 100) = 63\%$ of the ^{14}C in the leaf tissue. Of the ^{14}C label present in the leaf tissue whence the vacuoles came, TLC analysis showed that some 72% was in *p*ABA-Glc (Fig. 5*B*, *right panel*). The average proportion of [^{14}C]*p*ABA-Glc in vacuoles may thus be estimated as $(100 \times 63/72) = 88\%$.

Assay of pABA-Glc Uptake by Mitochondria—[^{3}H]*p*ABA-Glc was prepared from [^{3}H]*p*ABA and UDP-glucose using purified UGT75B1 to catalyze the reaction. The procedure (see "Experimental Procedures") gave an overall radiochemical yield of 18%. The [^{3}H]*p*ABA-Glc was supplied to purified cauliflower mitochondria energized with NADH; no uptake was detectable (Fig. 5*D*). The mitochondrial preparations were confirmed to be transport-competent by supplying [^{3}H]proline in place of [^{3}H]*p*ABA-Glc (Fig. 5*D*); proline is known to be readily taken up by energized plant mitochondria (31).

DISCUSSION

Humans and other higher animals do not synthesize folates *de novo* and therefore need a dietary supply that is mainly provided by plants. For this reason, there is considerable interest in engineering food plants for enhanced folate content (2, 4). To achieve this goal, the biosynthesis and metabolism of folates and their precursors need to be more fully understood (4).

In this study, we focused on the *p*ABA moiety of the folate molecule. It is well established that *p*ABA is made in the chloroplast, but is incorporated into folate in the mitochondrion (Fig. 1*B*). Until recently, there was a tacit assumption that *p*ABA principally existed as the free acid in plant cells. However, the major form of *p*ABA was found to be the D-glucopyranosyl ester, and plant extracts contained an enzyme activity that readily glucosylated *p*ABA (6). These findings raised the possibility *p*ABA-Glc could be the metabolite that is imported into the mitochondrion during folate synthesis. Alternatively, formation of the glucose ester could represent a mechanism of metabolite homeostasis, decreasing free *p*ABA levels in the cytosol through vacuolar sequestration of the glucosylated molecule.

The data presented here strongly favor the second possibility, for they demonstrate that the majority of *p*ABA-Glc in leaves is located in the vacuole, and that mitochondria do not import *p*ABA-Glc.

The evidence for a vacuolar location was both indirect and direct. Our K_{eq} value for *p*ABA glucose ester formation (3×10^{-3}) shows that the equilibrium disfavors product formation. Combining this K_{eq} value with literature data on UDP-glucose/UDP ratios in plant cytosol allows calculation of the cytosolic *p*ABA-Glc/*p*ABA-Glc ratio. Cytosolic UDP-glucose/UDP ratios in plant tissues are generally 10–20, the value reported for leaves being 13 (32–34). Using the value of 13 and a K_{eq} value of 3×10^{-3} gives a *p*ABA-Glc/*p*ABA ratio of 0.04, so that 96% of the total *p*ABA in the cytosol is predicted to be free and only 4% esterified. This calculated situation in the cytosol is opposite to results of whole tissue analysis, which show *p*ABA-Glc to be far more abundant than free *p*ABA in wild-type *Arabidopsis* and pea leaves (Fig. 4*E* and Refs. 6 and 14). This discrepancy implies that the bulk of the *p*ABA-Glc cannot be in the cytosol where *p*AGT activity resides (6) but must be sequestered elsewhere, most probably in the vacuole.

Direct experimental evidence for a predominantly vacuolar location for *p*ABA-Glc came from our dual-labeling tracer studies of pea leaf protoplasts and vacuoles, which showed that at least 88% of recently synthesized [^{14}C]*p*ABA-Glc is compartmented in vacuoles *in vivo*. This result accords with the deduction from tissue culture data (6, 9) that *p*ABA-Glc must be at least partly vacuolar. It is also in agreement with reports of

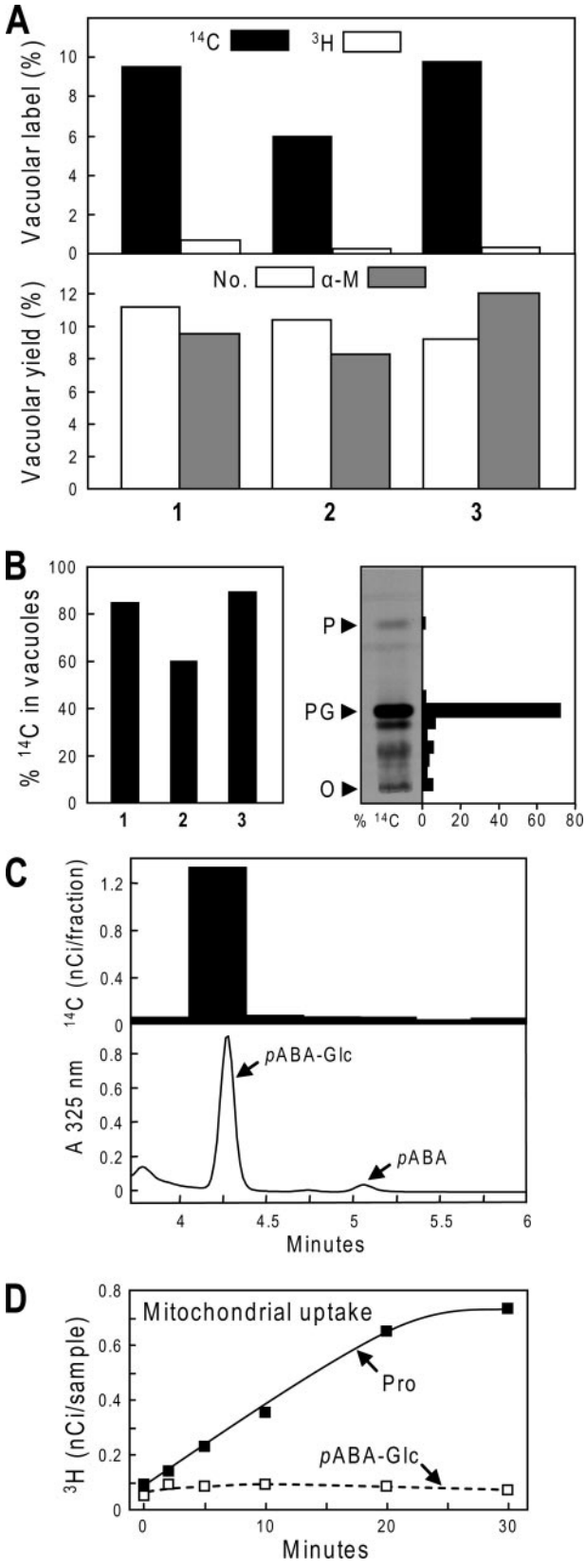

FIGURE 5. **Tests for *p*ABA-Glc uptake by vacuoles and mitochondria.** *A*, quantification of *in vivo* vacuolar accumulation of [^{14}C]*p*ABA-Glc. Pea leaflets (1 g) were supplied with [^{14}C]*p*ABA (118 nmol, 6.5 μCi) for 3 h, then mixed with 24 g of unlabeled leaves for protoplast preparation. Purified mesophyll protoplasts were osmotically lysed to liberate vacuoles, at which point low specific activity [^{3}H]folic acid was added; vacuoles were then isolated by Ficoll density gradient centrifugation. The ^{14}C and ^{3}H contents of the purified vacuole fraction were quantified and expressed as percentages of those of the protoplast lysate (*upper panel*). Vacuolar yields were estimated by counting vacuole numbers (*No.*) and from α-mannosidase activities (α-*M*) (*lower panel*). Results are from three independent experiments (*1–3*). *B*, *left panel*: The estimated percentage of ^{14}C label that was in vacuoles *in vivo*, in experiments *1–3*. Values were calculated from the data of *A* using the formula: 100 $\times$ (% vacuolar ^{14}C $-$ % vacuolar ^{3}H)/mean % vacuolar yield. Mean % vacuolar yield was based on the estimates from counting and α-mannosidase activity. *Right panel*, TLC separation of ^{14}C-labeled metabolites in pea leaflets supplied for 8 h with the same [^{14}C]*p*ABA dose given to leaflets used to prepare vacuoles. After the autoradiograph on the left was taken, the ^{14}C contents of TLC zones were determined, and expressed as percentages of the total ^{14}C label on the plate. The *p*ABA-Glc zone (*PG*) contained 72% of the total label. *O*, TLC origin; *P*, *p*ABA zone. *C*, co-chromatography of the ^{14}C label recovered from vacuoles with *p*ABA-Glc. A sample of the vacuole fraction was freed of Ficoll by ultrafiltration, mixed with authentic *p*ABA-Glc and *p*ABA standards, and separated by HPLC. The *p*ABA-Glc zone contained 80% of the total ^{14}C in the sample. *D*, lack of uptake of [^{3}H]*p*ABA-Glc by transport-competent cauliflower floret mitochondria. Purified mitochondria (0.33 mg protein) were incubated at 30 °C in a 0.5-ml reaction mixture containing 1 mM NADH and 7 nM [^{3}H]*p*ABA-Glc (92 nCi) or [^{3}H]proline (254 nCi). Samples (75 μl) were removed at the intervals shown; mitochondria were recovered by filtration on nitrocellulose membranes, which were assayed for ^{3}H. Data points are means of duplicate samples. The experiment was repeated, with similar results.

other aromatic Glc esters in plant vacuoles (35, 36) and, more generally, with the observation that many UGT reaction products accumulate in vacuoles (37). Thus, the fact that *p*ABA-Glc is rapidly cleared from the cytosol makes it an unlikely candidate for transport into mitochondria, and indeed our experiments failed to show mitochondrial *p*ABA-Glc uptake.

Interestingly, in leaves of *Arabidopsis* plants 95% of *p*AGT activity was associated with a single peak separated by anion exchange chromatography. The K_m value (0.12 mM) for this enzyme was found to be identical to that of a recombinant protein, UGT75B1, which we identified from a screen of 16 UGTs from a phylogenetic group of *Arabidopsis* enzymes previously shown to form glucose esters with benzoate and phenylpropanoid scaffolds. Knocking out the expression of UGT75B1, led to loss of ~95% of *p*AGT activity in the mutant, suggesting UGT75B1 encodes the activity observed in *Arabidopsis* extracts.

In an earlier study, UGT75B1 was found associated with the cell plate at cytokinesis but was distributed throughout cells that were not dividing (38). Because *p*ABA-Glc is in effect an activated form of glucose (6), our biochemical findings suggest the possibility that UGT75B1 functions at the cell plate by providing activated glucose units for the synthesis of a glucose polymer. Alternatively, *p*ABA-Glc could serve as a primer for such a polymer, analogous to the hydrophobic glycosides that function as primers in the synthesis of cellulose and other polysaccharides (39). In our present study and a previous one on pea (6) *p*AGT enzyme activity was located in the soluble fraction. This contrasts with the data from the cell plate study in which most of the UGT75B1 protein (detected immunologically) was recovered in a 100,000 $\times$ *g* pellet (38). However, the extraction buffer differed from ours in having less 2-mercaptoethanol (2 mM *versus* 10 mM) and in lacking polyvinylpolypyrrolidone (38). Both differences generally favor cross-linking and precipitation of proteins by phenols (40) and for polyvinylpolypyrrolidone this has been demonstrated in *Arabidopsis* (41). Moreover, tests showed that omitting polyvinylpolypyrrolidone from our extraction buffer and cutting the 2-mercapto-

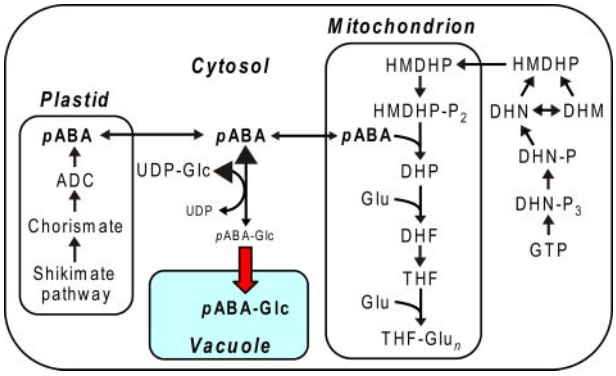

FIGURE 6. **An updated scheme of the plant folate synthesis pathway.** *Large arrowheads* in the *p*ABA ⇆ *p*ABA-Glc reaction indicate that the equilibrium strongly favors *p*ABA. The *bold red arrow* denotes *p*ABA-Glc import into the vacuole, presumably via a transporter. Mobilization of vacuolar *p*ABA-Glc would require reversal of this transport step or intravacuolar hydrolysis of *p*ABA-Glc.

ethanol concentration to 2 mM reduced the *p*AGT activity extracted from leaves by 78%. Dissimilar extraction conditions may thus account for the dissimilar results on localization.

In conclusion, our data clearly indicate the existence of a large vacuolar pool of *p*ABA-Glc. It is probable that this represents a readily reclaimable storage depot for *p*ABA moieties (6). The central vacuole in plant cells contains pools of many primary and secondary metabolites, frequently in conjugated forms, for which there are transport systems in the vacuolar membrane (35). Thus the occurrence of a vacuolar pool of a glucose conjugate and a cytosolic pool of free *p*ABA conforms to a very common pattern: a large storage pool of a metabolite in the vacuole, and a much smaller active metabolic pool in another subcellular compartment (42). Another possible function of the vacuolar pool of *p*ABA-Glc is as a pivotal part of a system to limit the concentration of free *p*ABA. As a hydrophobic weak acid, *p*ABA is able to diffuse back and forth across membranes, and hence to act as an uncoupler by collapsing electrochemical proton gradients (6, 43). High concentrations of *p*ABA could therefore in some circumstances have deleterious consequences, which are avoided by esterification with glucose and transporting the ester into the vacuole. A further reason to esterify and sequester *p*ABA may be that, at μM levels, it is a substrate inhibitor of dihydropteroate synthase, the enzyme that couples *p*ABA to pterin during folate synthesis (44, 45).

Finally, our data indicate that the current map of the folate synthesis pathway (*e.g.* 4) needs to be modestly redrawn, in its *p*ABA branch (Fig. 6). Specifically: in the *p*ABA ⇆ *p*ABA-Glc equilibrium in the cytosol, *p*ABA predominates; and *p*ABA-Glc is transported into (and stored in) the vacuole. Because *p*ABA-Glc is located in the vacuole, it is evident that mobilizing it would involve either export from the vacuole coupled with reversal of the synthesis reaction, or intravacuolar hydrolysis of *p*ABA-Glc. Such hydrolysis would presumably require a vacuolar esterase (6).

Acknowledgments—We thank Dr. Yair Shachar-Hill for helpful discussions about cytosolic concentrations of UDP-glucose and UDP and Michael J. Ziemak for technical assistance.

REFERENCES

1. Hanson, A. D., and Roje, S. (2001) *Annu. Rev. Plant Physiol. Plant Mol. Biol.* **52,** 119–137
2. Scott, J., Rébeillé, F., and Fletcher, J. (2000) *J. Sci. Food Agric.* **80,** 795–824
3. Hanson, A. D., and Gregory, J. F., 3rd (2002) *Curr. Opin. Plant Biol.* **5,** 244–249
4. Bekaert, S., Storozhenko, S., Mehrshahi, P., Bennett, M. J., Lambert, W., Gregory, J. F., 3rd, Schubert, K., Hugenholtz, J., Van Der Straeten, D., and Hanson, A. D. (2008) *Trends Plant Sci.* **13,** 28–35
5. Sterling, T. M., Balke, N. E., and Silverman, D. S. (1990) *Plant Physiol.* **92,** 1121–1127
6. Quinlivan, E. P., Roje, S., Basset, G., Shachar-Hill, Y., Gregory, J. F., 3rd, and Hanson, A. D. (2003) *J. Biol. Chem.* **278,** 20731–20737
7. Haferkamp, I. (2007) *FEBS Lett.* **581,** 2375–2379
8. Rea, P. A. (2007) *Annu. Rev. Plant Biol.* **58,** 347–375
9. Panjaitan, T. S., Syahrani, A., and Indrayanto, G. (2000) *J. Planar Chromat.-Modern TLC* **13,** 114–118
10. Ross, J., Li, Y., Lim, E., and Bowles, D. J. (2001) *Genome Biol.* **2,** reviews 3004.1–3004.6
11. Lim, E. K., Doucet, C. J., Li, Y., Elias, L., Worrall, D., Spencer, S. P., Ross, J., and Bowles, D. J. (2002) *J. Biol. Chem.* **277,** 586–592
12. Goulard, F., Diouris, M., Deslandes, E., and Floc'h, J. Y. (1999) *Eur. J. Phycol.* **34,** 21–25
13. Gibeaut, D. M., Hulett, J., Cramer, G. R., and Seemann, J. R. (1997) *Plant Physiol.* **115,** 317–319
14. Orsomando, G., Bozzo, G. G., de la Garza, R. D., Basset, G. J., Quinlivan, E. P., Naponelli, V., Rébeillé, F., Ravanel, S., Gregory, J. F., 3rd, and Hanson, A. D. (2006) *Plant J.* **46,** 426–435
15. Edwards, K., Johnstone, C., and Thompson, C. (1991) *Nucleic Acids Res.* **19,** 1349
16. Lim, E. K., Roberts, M. R., and Bowles, D. J. (1998) *J. Biol. Chem.* **273,** 34920–34925
17. Rohman, M., and Harrison-Lavoie, K. J. (2000) *Protein Expr. Purif.* **20,** 45–47
18. Bradford, M. M. (1976) *Anal. Biochem.* **72,** 248–524
19. Laemmli, U. K. (1970) *Nature* **227,** 680–685
20. Orsomando, G., de la Garza, R. D., Green, B. J., Peng, M., Rea, P. A., Ryan, T. J., Gregory, J. F., 3rd, and Hanson, A. D. (2005) *J. Biol. Chem.* **280,** 28877–28884
21. Bozzo, G. G., Basset, G. J., Naponelli, V., Noiriel, A., Gregory, J. F., 3rd, and Hanson, A. D. (2008) *Phytochemistry* **69,** 29–37
22. Nok, A. J., Shuaibu, M. N., Kanbara, H., and Yanagi, T. (2000) *Parasitol Res.* **86,** 923–928
23. Trossat, C., Nolte, K. D., and Hanson, A. D. (1996) *Plant Physiol.* **111,** 965–973
24. Douce, R., Bourguignon, J., Brouquisse, R., and Neuburger, M. (1987) *Methods Enzymol.* **148,** 403–415
25. Goldraij, A., and Polacco, J. C. (2000) *Planta* **210,** 652–658
26. Kocsis, M. G., Ranocha, P., Gage, D. A., Simon, E. S., Rhodes, D., Peel, G. J., Mellema, S., Saito, K., Awazuhara, M., Li, C., Meeley, R. B., Tarczynski, M. C., Wagner, C., and Hanson, A. D. (2003) *Plant Physiol.* **131,** 1808–1815
27. Winter, H., Robinson, D. G., and Heldt, H. W. (1994) *Planta* **193,** 530–535
28. Offen, W., Martinez-Fleites, C., Yang, M., Kiat-Lim, E., Davis, B. G., Tarling, C. A., Ford, C. M., Bowles, D. J., and Davies, G. J. (2006) *EMBO J.* **25,** 1396–1405
29. Li, L., Modolo, L. V., Escamilla-Trevino, L. L., Achnine, L., Dixon, R. A., and Wang, X. (2007) *J. Mol. Biol.* **370,** 951–963
30. Boller, T., and Kende, H. (1979) *Plant Physiol.* **63,** 1123–1132
31. Elthon, T. E., Stewart, C. R., and Bonner, W. D. (1984) *Plant Physiol.* **75,** 951–955
32. Dancer, J., Neuhaus, H. E., and Stitt, M. (1990) *Plant Physiol.* **92,** 637–641
33. Dancer, J., Veith, R., Feil, R., Komore, E., and Stitt, M. (1990) *Plant Sci.* **66,** 59–63
34. Farré, E. M., Tiessen, A., Roessner, U., Geigenberger, P., Trethewey, R. N., and Willmitzer, L. (2001) *Plant Physiol.* **127,** 685–700
35. Wink, M. (1997) in *The Plant Vacuole: Advances in Botanical Research,*

Vol. 25 (Leigh, R. A., Sanders, D., and Callow, J. A., eds), pp. 141–170, Academic Press, London, UK
36. Martinoia, E., Klein, M., Gessler, M., Sánchez-Fernández, R., and Rea, P. A. (2001) in *Vacuolar Compartments, CRC Series* (Robinson, D., and Rogers, J. eds), pp. 221–253, Sheffield Academic Press, Sheffield, UK
37. Bowles, D., Lim, E.-K., Poppenberger, B., and Vaistij, F. V. (2006) *Annu. Rev. Plant Biol.* **57,** 567–597
38. Hong, Z., Zhang, Z., Olson, J. M., and Verma, D. P. (2001) *Plant Cell* **13,** 769–779
39. Peng, L., Kawagoe, Y., Hogan, P., and Delmer, D. (2002) *Science* **295,** 147–150
40. Loomis, W. D., and Bataille, J. (1966) *Phytochemistry* **5,** 423–438
41. Charmont, S., Jamet, E., Pont-Lezica, R., and Canut, H. (2005) *Phytochemistry* **66,** 453–461
42. Lips, S. H., and Beevers, H. (1966) *Plant Physiol.* **41,** 709–712
43. Cohen, F. S., Eisenberg, M., and McLaughlin, S. (1977) *J. Membr. Biol.* **37,** 361–396
44. Hampele, I. C., D'Arcy, A., Dale, G. E., Kostrewa, D., Nielsen, J., Oefner, C., Page, M. G., Schonfeld, H. J., Stuber, D., and Then, R. L. (1997) *J. Mol. Biol.* **268,** 21–30
45. Rébeillé, F., Macherel, D., Mouillon, J. M., Garin, J., and Douce, R. (1997) *EMBO J.* **16,** 947–957